Phase transition between synchronous and asynchronous updating algorithms

Filippo Radicchi, Daniele Vilone, and Hildegard Meyer-Ortmanns
*School of Engineering and Science, International University Bremen * , P.O.Box 750561 , D-28725 Bremen , Germany.*

We update a one-dimensional chain of Ising spins of length L with algorithms which are parameterized by the probability p for a certain site to get updated in one time step. The result of the update event itself is determined by the energy change due to the local change in the configuration. In this way we interpolate between the Metropolis algorithm at zero temperature for p of the order of $1/L$ and for large L, and a synchronous deterministic updating procedure for $p = 1$. As function of p we observe a phase transition between the stationary states to which the algorithm drives the system. These are non-absorbing stationary states with antiferromagnetic domains for $p > p_c$, and absorbing states with ferromagnetic domains for $p \leq p_c$. This means that above this transition the stationary states have lost any remnants to the ferromagnetic Ising interaction. A measurement of the critical exponents shows that this transition belongs to the universality class of parity conservation.

PACS numbers: 05.70.Ln , 05.50.+q , 64.90.+b

The issue of synchronous versus asynchronous updating algorithms has attracted much attention in connection with Boolean networks [1, 2, 3, 4, 5], neural networks [6, 7], biological networks [8] and game theory [9, 10]. In a synchronous updating scheme all the units of the system are updated at the same time. Asynchronous updating usually means that not all units are updated at the same time. The algorithm can be asynchronous in the sense that each unit is updated according to its own clock, as in distributed systems for parallel processing [11], or it is asynchronous in the sense that only one randomly chosen unit is updated at each step, as in Monte Carlo algorithms [12]. In the context of thermal equilibrium dynamics updating algorithms like the Metropolis algorithm [13] are designed in a way that they drive the configurations to a set that is representative for the Boltzmann equilibrium distribution. The dynamics of the algorithm then enters only in an intermediate step, it is not representative for the intrinsic dynamics of the system that is determined by the Hamiltonian. In out-of-equilibrium systems the updating scheme may play a more prominent role. The number of attractors in Boolean networks, for example, increases exponentially with the system size [14] for synchronous update, and with a power for critical Boolean networks [15] for asynchronous update. The phase diagrams of the Hopfield neural network model [6, 16] and the Blume-Emery-Griffiths model [17, 18] depend on the updating mode as well, while those of the Q-state Ising model [19] and the Sherrington-Kirkpatrick spin glass [20] are independent on the used scheme.
Probably neither a completely synchronous nor a random asynchronous update is realistic for natural systems. Here we interpolate between these two extreme cases not in a more realistic way, but in a way that allows to identify a phase transition between the stationary states. We focus our attention on a one-dimensional Ising model at zero temperature. We visit all the sites and select each of them with probability p. Then we update simultaneously each of the selected candidates by flipping their spins if the local energy of the system is not increased due to this change. Tuning the value of p, we are able to interpolate the algorithm from an asynchronous one, in the thermodynamical limit corresponding to the Metropolis algorithm, to a synchronous one. We observe a phase transition between the stationary states from non-absorbing for $p > p_c$ to absorbing ones for $p \leq p_c$, with p_c the critical threshold of the transition. The time evolution of the Ising chain can be represented as a directed percolation (DP) process if bonds between spins of opposite signs are called active. As our measurements of the critical exponents show, the transition between these stationary states belongs to the universality class of parity conservation (PC).

We consider a one-dimensional lattice of length L. To each site i, $i = 1, \ldots, L$ of this chain we assign a spin variable σ_i, where σ_i takes the values $+1$ or -1. The Hamiltonian of the system is given by $H = -J \sum_{i=1}^{L} \sigma_i \sigma_{i+1}$, where J is the coupling constant between neighboring sites. Here we consider ferromagnetic couplings so that $J = 1$. Moreover, for definiteness we choose periodic boundary conditions so that $\sigma_{L+1} = \sigma_1$. The results will not depend on this choice.
A standard local stochastic updating algorithm for studying thermodynamic equilibrium of the Ising model is the Metropolis algorithm [12, 13, 21]. Given a configuration of the system $\Sigma(t) = \{\sigma_i(t)\}$ at time

*Jacobs University Bremen as of spring 2007

t, we pick up one site j at random and flip its spin with probability $P_j(t) = \min\{1, \exp[-\beta \Delta E_j(t)]\}$. Here $\beta = 1/kT$, with k the Boltzmann constant and T the temperature, while $\Delta E_j(t) = 2\sigma_j(t)[\sigma_{j-1}(t) + \sigma_{j+1}(t)]$ is the difference in energy that a flip of σ_j would induce. In particular, for zero temperature an increase in energy of the resulting configuration is always rejected. After the single update of the j-th site the time increases by $t \to t + 1/L = t'$ (and L single updates are considered as one time unit). The new configuration is given by $\Sigma(t') = \{\sigma_i(t); \sigma_j(t')\}$, where all sites $i \neq j$ have the same spin value as they have at time t, but only the spin of the j-th site is eventually flipped. It is well known that the Metropolis algorithm drives our chain of Ising spins to the Boltzmann equilibrium distribution for a sufficiently large number of update events. In the context here we emphasize that the Metropolis algorithm is fully asynchronous in the sense that we have only one spin flip per single update event.

Here we are no longer interested in the equilibrium properties of the Ising model, but in the algorithmic dynamics applied to Ising spins. Therefore we give up the asynchrony of the algorithm. Given the configuration $\Sigma(t) = \{\sigma_i(t)\}$ at time t, we visit all sites and select each of them with probability p. The selected sites are $j_1, \ldots, j_m$ and m, the total number of selected sites, is a random integer obeying the binomial distribution $B(m, L, p) = \binom{L}{m} p^m (1-p)^{L-m}$. Each of the m selected sites is then updated according to the Metropolis rule at temperature zero, so that the spin of the j_v-th site is flipped with probability $P_{j_v}(t)$, $\forall\, v = 1, \ldots, m$. After one step of the algorithm, the time increases as $t \to t + p = t'$, and the new configuration is $\Sigma(t') = \{\sigma_i(t); \sigma_{j_1}(t'); \ldots; \sigma_{j_m}(t')\}$, where all sites $i \neq j_1, \ldots, j_m$ have the same spin value as they have at time t, while the spins of the m selected sites are eventually flipped. One time unit has passed when the average number of update events equals to the total number of sites L. By varying p we can "tune" the algorithm from asynchrony, for p of order of $1/L$, to synchrony, for $p = 1$. In particular, for p of the order of $1/L$ and for sufficiently large values of L we recover the usual Metropolis algorithm when two or more simultaneous selections which occur with probability at most of the order of $1/L^2$ become negligible. We stress the fact that the spin value of the selected sites $j_1, \ldots, j_m$ at time t' is eventually flipped according to the actual values of the spins at time t, so that they depend only on the configuration $\Sigma(t)$. Differently from the standard Metropolis algorithm at zero temperature, for general values of p, the total energy of the new configuration $\Sigma(t')$ can be increased with respect to the total energy of the old configuration $\Sigma(t)$. Moreover, the long-time configurations $\Sigma(t \to \infty)$ do no longer obey the Boltzmann distribution.

In this paper, for simplicity, we focus on the case of zero temperature. The equilibrium ground-state of the one-dimensional Ising ferromagnet at zero temperature is one of the two ferromagnetic states with all spins positive or negative. In contrast, the completely synchronized dynamics does not drive the system to the ground state, but acts as parallel algorithm and amounts to a deterministic map T: $\Sigma(t+1) = T\Sigma(t)$, for all t. After a transient time $t_0 \leq L/2$, the algorithm drives the system into a cycle of length two [19], where the system "flips" between two configurations, $\Sigma_1 = \{^1\sigma_i\}$ and $\Sigma_2 = \{^2\sigma_i\}$, such that $\Sigma_2 = T\Sigma_1$ and $\Sigma_1 = T\Sigma_2$, for all $t \geq t_0$. In particular, these configurations result from each other by an overall flip of signs in the sense that $\Sigma_2 = \{-\,^1\sigma_i\}$ and $\Sigma_1 = \{-\,^2\sigma_i\}$. Moreover, these states are anti-ferromagnetic because we observe domains (neighboring sites with the same value of the spin) of a length of at most two sites. Therefore, it is natural to study intermediate values of p, in particular to focus on the transition between the ferromagnetic and the anti-ferromagnetic configurations of the final state.

Let us consider the active bonds of the system, where we define a bond as active if it connects two sites with opposite spins. As remnant of the zero-temperature Ising model only sites belonging to at least one active bond can flip and do flip if they are selected as candidates for the updating. Only a few elementary processes, that involve active bonds, can take place: diffusion, annihilation and creation. For clarity of notation, let us indicate as $\uparrow$ a site with positive spin and as $\downarrow$ a site with negative spin. Consider, for example, a local configuration such as $\cdots\uparrow\uparrow\downarrow\downarrow\cdots$ at time t: at time $t+p$ it can evolve to $\cdots\uparrow\uparrow\uparrow\downarrow\cdots$ or to $\cdots\uparrow\downarrow\downarrow\downarrow\cdots$, depending on whether they are selected for update that happens with probability $2p(1-p)$ [diffusion], or to $\cdots\uparrow\downarrow\uparrow\downarrow\cdots$ with probability p^2 [creation], or it remains unchanged with probability $(1-p)^2$. Using the same rules, a local configuration such as $\cdots\uparrow\uparrow\downarrow\uparrow\uparrow\cdots$ at time t later, at time $t+p$, can become $\cdots\uparrow\downarrow\uparrow\downarrow\uparrow\cdots$ with probability p^3 [creation], or $\cdots\uparrow\uparrow\uparrow\uparrow\uparrow\cdots$ with probability $p(1-p)^2$ [annihilation], etc. ... It is easily checked that the parity of active bonds, that is the number of active bonds modulo 2, is conserved.

The former considerations suggest that the transition between ferromagnetic and anti-ferromagnetic behavior (without active bonds and with dominance of active bonds, respectively) is given by the competition of annihilation and creation of active bonds. In particular, the creation is favored by a synchronous updating scheme, because a new couple of active bonds can be created only if two neighboring sites simultaneously flip their spins. Therefore the transition between stationary states (ferromagnetic and anti-ferromagnetic ones) can be considered as a transition between the asynchronous/synchronous updating schemes. Furthermore, this transition corresponds to a $(1+1)$-dimensional DP transition [22, 23]. The active bonds correspond

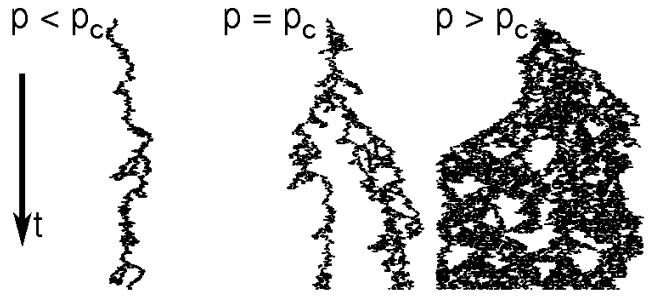

Figure 1: Evolution of an isolated active bond in the subcritical, critical and supercritical regimes. We show only the part around the initial active bond. From left to right: $p = 0.39$, $p = 0.41 = p_c$, $p = 0.43$.

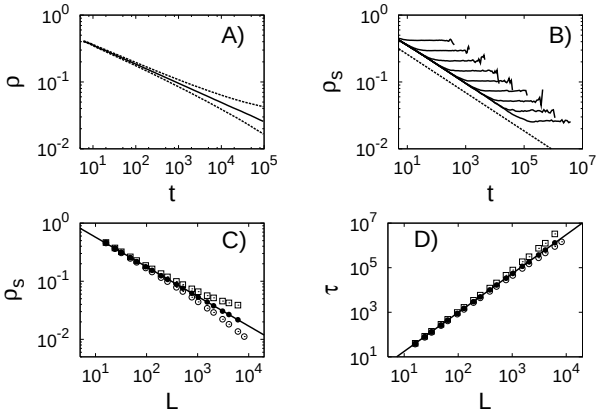

Figure 2: **A)** Time decay of the density of active bonds ρ in the subcritical ($p = 0.40$), critical ($p = 0.41 = p_c$) and supercritical ($p = 0.42$) regime, from bottom to top, respectively. **B)** Average density of active bonds ρ_s surviving up to time t over samples, plotted as a function of time at the critical point for $L = 16, 32, 64, 128, 256, 512, 1024, 2048, 4096$ and 6144, from top to bottom respectively. The dotted line has a slope of $-\delta = -0.286(1)$. **C)** Average density of active sites over the surviving samples ρ_s as a function of size L of the lattice for $p = 0.40$ (empty dots) 0.41 (full dots) and 0.42 (empty squares). The full line has slope $-\beta/\nu_\perp = -0.51(1)$. **D)** Average relaxation time τ as a function of the size L of the lattice for $p = 0.40$, 0.41 and 0.42 [the symbols are the same as in C)]. The full line has slope $z = \nu_\parallel/\nu_\perp = 1.746(2)$.

to the occupied sites in DP. A qualitative picture of this transition is shown in Figure 1. We plot the time evolution of an isolated active bond (that is not the only one in the system) for three different values of p. We only display the intermediate part of the lattice around the initial active bond. The initial configuration is chosen as $\cdots \uparrow\uparrow\downarrow\downarrow \cdots$. In the subcritical regime $p < p_c$, the initial active bond will remain alone for most of the time, diffusing, and, from time to time, creating couples of new active bonds which annihilate soon. In the supercritical regime $p > p_c$, the average number of creations is larger than the average number of annihilations, so that the active bonds spread over the entire system. In the critical regime $p = p_c$, annihilation and creation processes are balanced and the active bonds do not spread over the system, but remain confined in a finite region leading to the same qualitative picture as we see in the subcritical region.

In order to obtain a quantitative description of the transition, we use as order parameter the density of active bonds ρ, given by the ratio of the number of active bonds and the total number of bonds in the lattice. The initial condition is always chosen as $\rho(0) = 1$, so that the lattice is fully occupied with active bonds. All data points are obtained from averaging over at least 10^3 realizations and up to 10^5 realizations for small sizes of the lattice. Here, these values of L are considered as the large-volume limit in the following. Let us first determine the critical probability p_c. In Figure 2A) we plot the time behavior of ρ for three different values of p and $L = 10^4$. As we can see, for $p = 0.41$ $\rho(t) \sim t^{-\delta}$ with $\delta = 0.286(1)$, while for $p = 0.40$ $\rho(t)$ decreases with negative curvature, for $p = 0.42$ $\rho(t)$ it increases with positive curvature. The positive curvature characterizes the different phase. Therefore, within the given accuracy, we locate the critical threshold p_c as the largest value such that the curvature is non-positive. In this way we obtain $p_c = 0.41(1)$ as the critical point. Determining p_c with higher precision would amount to an increase in the linear size of the lattice L and the time for observing the positive curvature of ρ. Here we do not perform this kind of computationally expensive simulations, but calculate the critical exponents without increasing the precision in p_c.

Critical exponents. Along the determination of p_c we have already read off the exponent δ from the time evolution of ρ: for $p < p_c$ and in the thermodynamic limit $L \to \infty$, we should observe $\rho(t) \sim t^{-\alpha(p)}$, with $\alpha(p)$ a continuous and monotonic decreasing function of p and enclosed by curves with $\alpha(p) = 1/2$ for $p \to 0^+$, as in the case of the standard Metropolis algorithm [12, 21], and $\alpha(p_c) = \delta$, as observed in our numerical simulation. Therefore, the negative curvature observed in the subcritical regime, is a finite-size effect. Also in the supercritical regime the curve bends down to zero as a finite-size effect after a sufficiently large time, but the positive curvature signals the onset of the new (supercritical) phase.

Finite-size scaling analysis. Finite-size effects in the density of active bonds are manifest in two ways: if we follow the time evolution of a certain configuration of a chain of length L, we observe a power-law decay of active bonds up to a certain time $t_d(L, p)$ for $p \leq p_c$. After that, either the density drops to zero faster than a power-law, this happens for most configurations, for which a fluctuation drives the system into the absorbing state, or, in the minority of evolutions, the number of

active bonds fluctuates around a plateau, before the plateau drops to zero in the end. Configurations of this minority are called *surviving* configurations up to time τ. Now it is easier to locate the onset of the plateau than the onset of a faster decay, and therefore to study the finite-size scaling of the density of active bonds ρ_s of surviving configurations as a function of L, averaged only over the surviving realizations [24]. In Figure 2B) we plot the time behavior of ρ_s at the critical point for several values of the size L. As we can see, after an initial transient in which ρ_s decreases as $t^{-\delta}$, it reaches a stationary value depending on L. This value vanishes in the thermodynamical limit, since the plateau is a finite-size effect. We average along the values of the plateau (since averaging over time and over different realizations are assumed to be equivalent), for different system sizes. In Figure 2C) this average value is plotted as a function of L for three values of p ($p = 0.40$, $p = 0.41 = p_c$ and $p = 0.42$). Again, at the critical point we find a power law decay $\rho_s \sim L^{-\beta/\nu_\perp}$, with $\beta/\nu_\perp = 0.51(1)$, while the decay deviates from the power-law behavior in both the subcritical and the supercritical regimes. (Here the exponent β characterizes the behavior of the order parameter $\bar{\rho}(p) \sim |p_c - p|^\beta$, $\nu_\perp$ the spatial correlation length $\xi(p) \sim |p_c - p|^{-\nu_\perp}$ both in the vicinity of p_c.) Moreover, from the finite-size scaling analysis we calculate the dynamical exponent $z = \nu_\parallel/\nu_\perp$, where $\nu_\parallel$ characterizes the time-like correlation length $\tau(p) \sim |p_c - p|^{-\nu_\parallel}$. The exponent z is derived from the relaxation time τ needed by a finite system to reach the absorbing configuration [$\rho(t \geq \tau) = 0$]. In Figure 2D) τ is plotted as a function of L for $p = 0.40$, $p = 0.41 = p_c$ and $p = 0.42$. At $p = p_c$ we find again a power-law dependence $\tau \sim L^z$, with $z = \nu_\parallel/\nu_\perp = 1.746(2)$, while for different values of p τ behaves differently from a power-law behavior, as it is seen in Figure 2D). Furthermore, in Figure 3 we verify the finite-size scaling relation $\rho(p_c, L, t) \sim L^{-\beta/\nu_\perp} f(t/L^z)$, where $f(\cdot)$ is a suitable universal function. Finally, we determine the static exponent γ from the growth of fluctuations in the order-parameter susceptibility, defined as $\chi = L(\langle\rho^2\rangle - \langle\rho\rangle^2)$, via $\chi_s \sim L^{\gamma/\nu_\perp}$ at p_c (where the index s again refers to an average over the surviving configurations). We find $\gamma \simeq 0$, but we do not report any figure here. We further determine the dynamical exponent η and check the exponents δ and z in the following way. Starting from a configuration like $\cdots \uparrow\uparrow\downarrow\uparrow\uparrow \cdots$, that is a ferromagnetic configuration with only two active bonds, we numerically compute the survival probability $P(t)$ (that is the probability that the system had not entered the absorbing state up to time t), the average number of active bonds $\bar{n}(t)$ and the average mean square distance of spreading $\bar{R}^2(t)$ from an arbitrary selected site. These quantities are expected to behave at the critical point p_c as $P(t) \sim t^{-\delta}$, $\bar{n}(t) \sim t^\eta$ and $\bar{R}^2(t) \sim t^{2/z}$ [22, 23, 24]. From these simulations we find

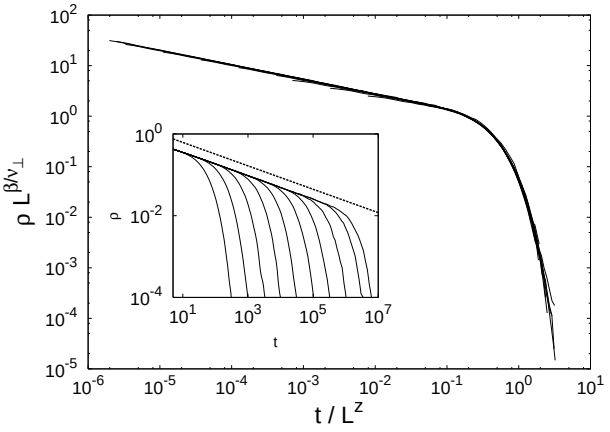

Figure 3: The main plot shows the finite-size scaling of the density of active bonds ρ. The inset shows the unscaled data, where the dotted line has a slope equal to $-\delta$. The datasets are the same as in Figure 2.

$\eta \simeq 0$ and values of δ and z consistent with the former ones within the error bars. The figures are not displayed.

In conclusion, we have calculated the static exponents $\beta/\nu_\perp = 0.51(1)$ and $\gamma \simeq 0$ and the dynamical exponents $\delta = 0.286(1)$, $\nu_\parallel/\nu_\perp = z = 1.746(2)$ and $\eta \simeq 0$. These values are consistent with the ones conjectured for the PC universality class $\beta/\nu_\perp = 1/2$, $\gamma = 0$, $\delta = 2/7$, $\nu_\parallel/\nu_\perp = 21/12$ and $\eta = 0$ [22, 23, 24, 25, 26, 27, 28, 29, 30]. This is expected because periodic boundary conditions for Ising spins as well as the updating rules we used preserve the parity of the number of active bonds, and for free boundary conditions only the boundaries may violate the conservation of parity which leads to a negligible effect. Even if parity is non-conserved as in case of the non-equilibrium kinetic Ising model [29, 30], for which spin-flip and spin-exchange dynamics are mixed, the PC universality class is observed. An increase in the dimensionality of the lattice would allow a mean-field description of the transition, since the PC universality class has the critical dimension $d_c = 2$ [22, 23]. Our preliminary numerical simulations for this case show qualitatively similar phases as in $d = 1$, but with the transition point shifted towards 1. Our work represents the first systematic interpolation between a synchronous and asynchronous updating scheme. The existence of a phase transition sheds some light on the interpretation of stationary states whenever they depend on the updating mode. Beyond the transition these states may have lost any remnants of the "intrinsic" dynamics (in our case the ferromagnetic Ising interaction). Instead, they are representative for the dynamics of the updating algorithm itself.

[1] S. A. Kauffman, J. Theor. Biol. **22**, 437 (1969).
[2] S. A. Kauffman, Nature (London) **224**, 177 (1969).
[3] K. Klemm and S. Bornholdt, arXiv.org:q-bio/0309013 (2003).
[4] K. Klemm and S. Bornholdt, Phys. Rev. E **72**, 055101 (2005).
[5] F. Greil and B. Drossel, Phys. Rev. Lett. **95**, 048701 (2005).
[6] J. J. Hopfield, Proc. Natl. Acad. Sci. USA **79**, 2554 (1982).
[7] R. O. Grondin, W. Porod, C. M. Loeffler, and D. K. Ferry, Biol. Cybern. **49**, 1 (1983).
[8] K. Klemm and S. Bornholdt, Proc. Natl. Acad. Sci. USA **102**, 18414 (2005).
[9] B. A. Huberman and N. S. Glance, Proc. Natl. Acad. Sci. USA **90**, 7716 (1993).
[10] H. J. Block and B. Bergersen, Phys. Rev. E **59**, 3876 (1999).
[11] E. Arjomandi, M. J. Fischer, and N. A. Lynch, J. ACM **30**, 449 (1983).
[12] M. E. J. Newman and G. T. Barkema, *Monte Carlo Methods in Statistical Physics* (Oxford University Press, Oxford, 1999).
[13] N. A. Metropolis *et al.*, J. Chem. Phys. **21**, 1087 (1953).
[14] B. Samuelsson and C. Troein, Phys. Rev. Lett. **90**, 098701 (2003).
[15] B. Drossel, T. Mihaljev, and F. Greil, Phys. Rev. Lett. **94**, 088701 (2005).
[16] J. F. Fontanari and R. Köberle, J. Physique **49**, 13 (1988).
[17] M. Blume, V.J. Emery, and R. B. Griffiths, Phys. Rev. A **4**, 1071 (1971).
[18] D. Bollé and J. Busquets Blanco, Eur. Phys. J. B **47**, 281 (2005).
[19] D. Bollé and J. Busquets Blanco, Eur. Phys. J. B **42**, 397 (2004).
[20] H.Nishimori, TITECH Report (1997) unpublished.
[21] V. Privman, *Nonequilibrium Statistical Mechanics in One Dimension*, (Cambridge University Press, Cambridge, 1997).
[22] H. Hinrichsen, Adv. Phys. **49**, 815 (200).
[23] G. Ódor, Rev. Mod. Phys. **76**, 663 (2004).
[24] I. Jensen, Phys. Rev. E **50**, 3623 (1994).
[25] I. Jensen, J. Phys. A: Math. Gen. **26**, 3921 (1993).
[26] D. ben-Avraham, F. Leyvraz, and S. Redner, Phys. Rev. E **50**, 1843 (1994).
[27] D. Zhong and D. ben-Avraham, Phys. Lett. A **209**, 333 (1995).
[28] H. K. Janssen, Phys. Rev. Lett. **78**, 2890 (1997).
[29] N. Menyhárd and G. Ódor, J. Phys. A: Math. Gen. **29**, 7739 (1996).
[30] N. Menyhárd and G. Ódor, Braz. J. Phys. **30**, 113 (2000).